Journal of Alloys and Compounds 509 (2011) 3886–3888

Contents lists available at ScienceDirect

Journal of Alloys and Compounds

journal homepage: www.elsevier.com/locate/jallcom

Enhanced red emission in $LiAl_5O_8$:Fe^{3+} phosphor by B^{3+} doping

Wei Shu[a,b], R.F. Qiang[a,b], Siguo Xiao[a,b,*], Xiaoliang Yang[a], J.W. Ding[a]

[a] Institute for Nanophysics and Rare-earth Luminescence, Xiangtan University, Xiangtan 411105, Hunan, China
[b] Key Laboratory of Quantum Engineering and Micro-Nano Energy Technology (Xiangtan University), Department of Education of Hunan Province, China

ARTICLE INFO

Article history:
Received 26 July 2010
Received in revised form
17 December 2010
Accepted 21 December 2010
Available online 28 December 2010

Keywords:
Flux
B^{3+}
Lifetime
Phosphor

ABSTRACT

Fe^{3+}, B^{3+} co-doping $LiAl_5O_8$ phosphor has been successfully synthesized by a solid-state reaction method assisted with wet chemical mixing route. Photoluminescence emission peak is observed at around 672 nm excited at both 290 nm ultraviolet and 565 nm green light. With introduction of a small amount of boric acid, the red emission intensity can be enhanced by 2.62 times under 290 nm excitation and 2.31 times under 565 nm excitation, respectively. It is believed that the substitution of B^{3+} ions for Al^{3+} sites decreases the symmetry of the luminescence center, intensifying the red emission.

1. Introduction

The Fe^{3+} doped $LiAl_5O_8$ has been studied for a long time because of its interesting optical properties [1–3]. In this phosphor, the Fe^{3+} ions could occupy the tetrahedral sites and the octahedral sites in the lattice [1]. Fe^{3+} has d^5 electronic configuration and thus its luminescence property involves the intraconfigurational d–d transitions [4]. In principle, the electric dipole transitions are both spin and parity forbidden. However, mixing of the opposite parity states by odd components of the crystal field violates the selection rules. As a result, the luminescence transition of Fe^{3+} in octahedral oxygen coordination will not easily take place because of its excellent symmetry. However, the Fe^{3+} doped $LiAl_5O_8$ exhibits a broad band emission with the peak at around 680 nm (deep red emitting), which might ascribe to the d–d transition of Fe^{3+} in tetrahedral oxygen coordination because the electric dipole selection rules is easy to be broken down due to its lower symmetry.

The deep red emission of the phosphor is useful in several applications, particularly in artificial illumination for plant growth and field emission displays [5,6]. Therefore, it is tremendously significant to enhance the luminous intensity of $LiAl_5O_8$:Fe^{3+} phosphor. Doping of B^{3+} in the matrix has been witnessed to be a feasible approach to enhance luminescence intensity in some aluminate-matrix phosphor, because boric acid can act as a flux to stimulate the lattice formation and grain growth [7–9]. More importantly, B^{3+} replacing Al^{3+} sites can decrease the symmetry of the luminescence center [10–12]. Thus boron doping into $LiAl_5O_8$:Fe^{3+} phosphor is worth considering.

In this paper, $LiAl_5O_8$:Fe^{3+} with different boric acid concentration is synthesized by a solid-state reaction method assisted with wet chemical mixing route. The luminescence mechanism, the effect of B^{3+} on the crystal structure and optical properties are discussed.

2. Experimental

The samples were prepared by a solid-state reaction method assisted with wet chemical mixing route. The staring materials were analytical reagent grade $LiNO_3$, $Al(NO_3)_3{\cdot}9H_2O$, and $FeCl_3{\cdot}6H_2O$, H_3BO_3. The samples were designed according to the stoichiometric balance molar composition of $LiAl_{4.999-x}O_8$:$Fe_{0.001}$, B_x (x = 0.01, 0.04, 0.06, 0.08, 0.10 and 0.12). Firstly, all the starting materials were dissolved into distilled water to obtain a homogeneous mixture. The thoroughly mixed solution was then transferred to a crucible and put into a muffle furnace, heated at 400 °C for 2 h. During this process, the solution was evaporated to dryness and decomposed into well mixed oxides. Then the powders were fired at 1200 °C for 10 h. After cooling to room temperature, white powders were obtained.

The powders were characterized by X-ray diffraction (XRD) on a Bruker D8 advance equipment using Cu tube with K_α radiation of 1.5406 Å in the 2θ range of 10–70°. The excitation and emission spectra and luminescence lifetime were measured by a spectrometer equipment (Model F-4500, Hitachi, Japan) with a 150 W xenon lamp as the excitation source. All measurements were performed at room temperature.

3. Results and discussion

In order to check crystal structure of the powder, the X-ray diffraction (XRD) patterns of $LiAl_{4.879}O_8$:$Fe_{0.001}$,$B_{0.12}$ and $LiAl_{4.999}O_8$:$Fe_{0.001}$ have been measured, shown in Fig. 1. As a com-

* Corresponding author at: Institute for Nanophysics and Rare-earth Luminescence, Xiangtan University, Xiangtan 411105, Hunan, China. Tel.: +86 13786239082.
E-mail address: xiaosiguo@xtu.edu.cn (S. Xiao).

0925-8388/$ – see front matter © 2011 Published by Elsevier B.V.
doi:10.1016/j.jallcom.2010.12.144

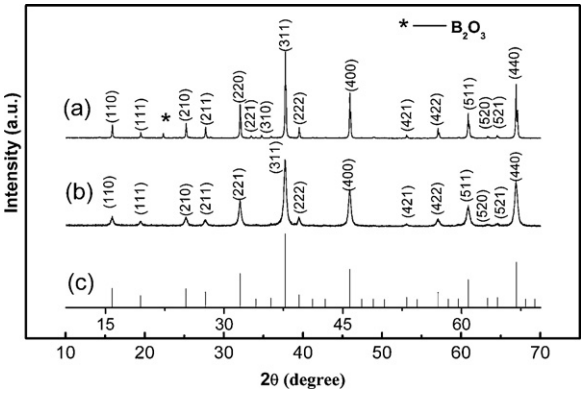

Fig. 1. XRD pattern of $LiAl_5O_8$ phosphor with different doping: (a) $LiAl_{4.879}O_8$:$Fe_{0.001}$,$B_{0.12}$, (b) $LiAl_{4.999}O_8$:$Fe_{0.001}$, (c) pure $LiAl_5O_8$ JCPDS, No. 87-1278).

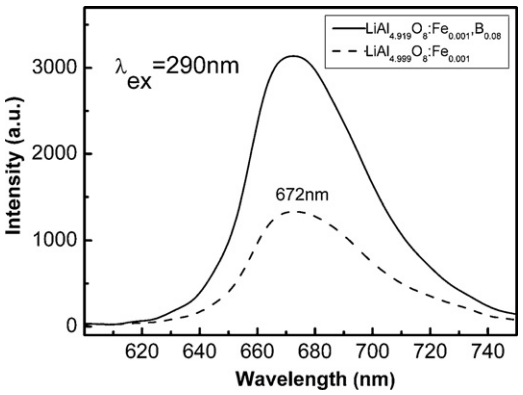

Fig. 3. Emission spectra (under 290 nm excitation) of $LiAl_{4.919}O_8$:$Fe_{0.001}$,$B_{0.08}$ and $LiAl_{4.999}O_8$:$Fe_{0.001}$ phosphor.

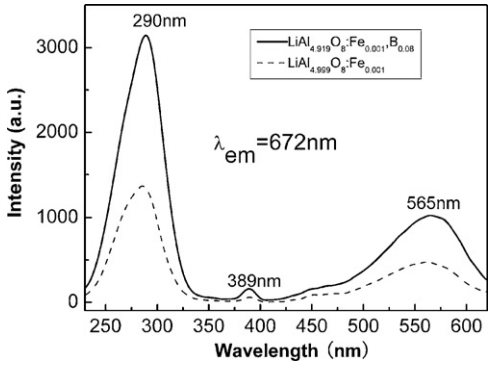

Fig. 2. Excitation spectra (monitored at 672 nm emission) of $LiAl_{4.919}O_8$:$Fe_{0.001}$,$B_{0.08}$ and $LiAl_{4.999}O_8$:$Fe_{0.001}$ phosphor.

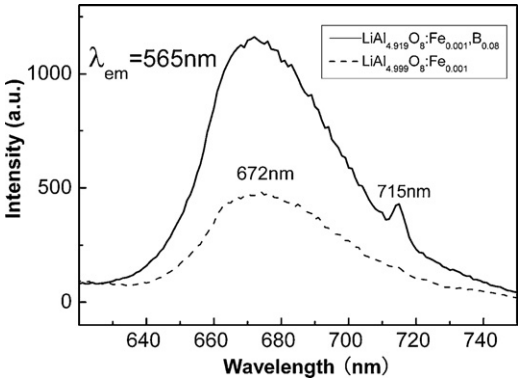

Fig. 4. Emission spectra (under 565 nm excitation) of $LiAl_{4.919}O_8$:$Fe_{0.001}$,$B_{0.08}$ and $LiAl_{4.999}O_8$:$Fe_{0.001}$ phosphor.

parison, a standard diffraction pattern for pure $LiAl_5O_8$ (JCPDS, No. 87-1278, $P4_332$, cubic, lattice parameters a = 7.9030 Å, cell volume = 493.60 Å^3) is also presented in Fig. 1. By analyzing these diffractive peaks, it is evident that the introduction of Fe^{3+} ions and B^{3+} ions (even at x = 0.12) does not change the main phase. The calculated lattice parameters are a = 7.9019 Å with cell volume = 493.3928 Å^3 for the $LiAl_{4.879}O_8$:$Fe_{0.001}$,$B_{0.12}$ sample and a = 7.9036 Å with cell volume = 493.7055 for the $LiAl_{4.999}O_8$:$Fe_{0.001}$ sample. According to vegard's rule, the lattice cell will be contracted when B^{3+} occupied Al^{3+} sites (ionic radius: $B^{3+} < Al^{3+}$) [13]. By the same token, when Fe^{3+} occupy Al^{3+} sites (ionic radius: $Fe^{3+} > Al^{3+}$), the lattice cell will be slightly expanded. The values of lattice parameters show the substitution complies with vegard's rule, revealing that Fe^{3+} and B^{3+} well substitute the Al^{3+} sites in the matrix.

The excitation and emission spectra of the $LiAl_{4.919}O_8$:$Fe_{0.001}$,$B_{0.08}$ and $LiAl_{4.999}O_8$:$Fe_{0.001}$ phosphor are illustrated in Figs. 2–4, respectively.

In Fig. 2, a strong excitation band at 290 nm for both $LiAl_{4.919}O_8$:$Fe_{0.001}$,$B_{0.08}$ and $LiAl_{4.999}O_8$:$Fe_{0.001}$ phosphor is measured, along with a moderately strong band at 565 nm and two weak bands at 389 nm and 450 nm. No excitation band shift is observed with the introduction of B^{3+} ions. However, the intensity of the excitation peak for the $LiAl_{4.919}O_8$:$Fe_{0.001}$,$B_{0.08}$ phosphor is 2.48 times stronger than that of the $LiAl_{4.999}O_8$:$Fe_{0.001}$ phosphor. The emission spectra (under 290 nm excitation) in Fig. 3 show a red emission band at 672 nm for both $LiAl_{4.919}O_8$:$Fe_{0.001}$,$B_{0.08}$ and $LiAl_{4.999}O_8$:$Fe_{0.001}$ phosphor. Similarly, no emission shift is observed with the introduction of B^{3+} ions. Yet the luminescence intensity for $LiAl_{4.919}O_8$:$Fe_{0.001}$,$B_{0.08}$ phosphor is 2.62 times stronger than that for the $LiAl_{4.999}O_8$:$Fe_{0.001}$ phosphor. The results

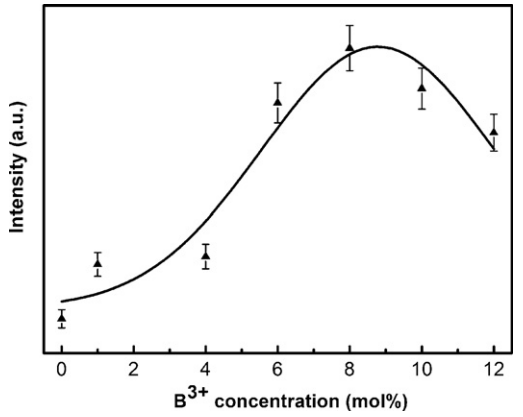

Fig. 5. Influence of B^{3+} concentration on the emission intensity of $LiAl_5O_8$:Fe^{3+} phosphor under 290 nm excitation.

suggest that B^{3+} doping can improve the ultraviolet-red conversion efficiency.

Fig. 5 further shows the emission intensity as a function of the B^{3+}. The emission intensity increases with the H_3BO_3 content, reaching a maximum at H_3BO_3 content of x = 0.08, and then decreases at higher H_3BO_3 content.

The emission spectra excited at 565 nm green light in Fig. 4 show strong emission bands at 672 nm of both $LiAl_{4.919}O_8$:$Fe_{0.001}$,$B_{0.08}$ and $LiAl_{4.999}O_8$:$Fe_{0.001}$ phosphor, which indicates the phosphor can also convert the green light into red light efficiently. As the green light fails to satisfy the photosynthesis of the plant, this conversion is meaningful, in that it can act as light conversion agent

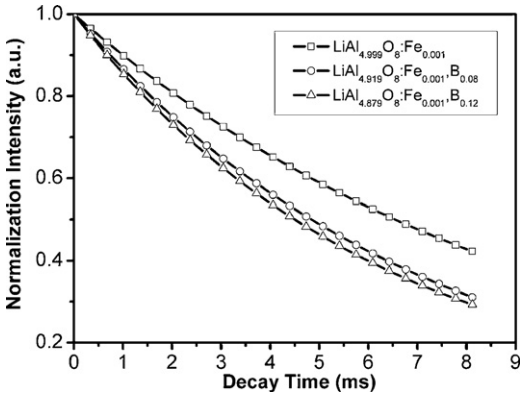

Fig. 6. Luminescence decay curves monitored at 672 nm of $LiAl_{4.919}O_8:Fe_{0.001},B_{0.08}$, $LiAl_{4.879}O_8:Fe_{0.001},B_{0.12}$ and $LiAl_{4.999}O_8:Fe_{0.001}$ phosphor.

for agricultural films and convert both ultraviolet and green light into red light, helping plants to enhance the utilization rate of sunlight. As shown in Fig. 4, the red emission at 672 nm for the $LiAl_{4.919}O_8:Fe_{0.001},B_{0.08}$ phosphor is 2.31 times stronger than that for the $LiAl_{4.999}O_8:Fe_{0.001}$ phosphor. This indicates that the B^{3+} doping can also enhance the conversion efficiency of the green light into red light.

Additionally, it is very interesting that emission spectra appear a very weak shoulder at 715 nm under 565 nm excitation. This emission is assigned to an unintentional Cr^{3+} impurity [14].

Traditionally, the strongest excitation band at 290 nm is assigned to the charge transfer of $Fe^{3+} \leftarrow O^{2-}$, and the moderately strong band at 565 nm maybe due to an overlapped of the prevalence of the (Fe^{3+}–V_O) defect complex and the internal transition on Fe^{3+} ions: $^6A_1(^6S) \rightarrow {}^4T_2(^4G)$, which are reported in previous papers [1,15]. The weak excitation bands are assigned to the internal transition on Fe^{3+} ion: 389 nm, $^6A_1(^6S) \rightarrow {}^4E(^4D)$, 450 nm, $^6A_1(^6S) \rightarrow {}^4T_2(^4D)$ [1,4]. The emission at 672 nm is assigned to the transition on the tetrahedral Fe^{3+} ion: $^4T_1(^4G) \rightarrow {}^6A_1(^6S)$ [1].

When H_3BO_3 is introduced as flux into the matrix, the synthesis temperature will decrease. H_3BO_3 facilitates the host-lattice formation and the grain growth. The co-doped B^{3+} ions can also substitute for the Al^{3+} sites, which are proved by IR and NMR measurement in previous papers [10,11]. Moreover, it might be helpful for the substitution of Fe^{3+} ions for Al^{3+} ions in the host lattice. As mentioned above, the lattice parameters decrease when B^{3+} ions occupies Al^{3+} sites, complying with vegard's rule [13]. The lattice contraction intensifies the crystal field and lowers the local symmetry of the luminescence centers, enhancing the luminescence emission [7]. In order to further verify this B^{3+}-doping effect, the lifetime for the 672 nm emission has been measured, shown in Fig. 6. The lifetime τ can be expressed as

$$\tau = \frac{1}{A + W_{NR}}, \quad (1)$$

where A is the rate of radiative transition probability, W_{NR} the rate of nonradiative transition probability. With B^{3+} ions substituting for the Al^{3+} sites, the symmetry of the luminescence center decreases. This results in the increase of the radiative transition probability A. At the meantime, the introduction of H_3BO_3 might also lead to the higher energy vibrational quanta around the luminescence center. Hence, the non-radiative transition probability W_{NR} will increase according to the non-radiative decay theory [16,17]. As a result, the introduction of H_3BO_3 leads to the decrease of the lifetime of the red emission. The shortened lifetime reveals the change of local environment of the luminescence center with the introduction of H_3BO_3.

The introduction of a small amount of H_3BO_3 helps more Fe^{3+} to enter the lattice sites, meaning that more Fe^{3+} can emit light. Moreover, it increases the radiative transition probability. Therefore, the red emission is finally intensified with the introduction of a small amount of H_3BO_3, although the non-radiative transition probability increases. However, when H_3BO_3 content exceeds 8 mol%, non-radiative energy transfers will result in the luminescence quenching.

4. Conclusions

Deep red emitting Fe^{3+}, B^{3+} co-doping $LiAl_5O_8$ phosphor is successfully synthesized by a solid-state reaction method assisted with wet chemical route. The luminescence is related to d–d transitions of Fe^{3+} in tetrahedral sites. The addition of H_3BO_3 not only acts as a flux, but also supplies cationic substitution to decrease the symmetry of the luminescence center and helps to form more luminescence centers, enhancing the luminescence emission. The optimal molar ratio of B^{3+} is 8 mol% $LiAl_5O_8:Fe^{3+}$ phosphor in the experiment.

Acknowledgements

This work was supported by Scientific Research Fund of Hunan Provincial Education Department (No. 10A120), Hunan Provincial Natural Science Foundation of China (No. 10JJ6012), and partially by the Key Laboratory of Quantum Engineering and Micro-Nano Energy Technology (Xiangtan University), Department of Education of Hunan Province, China (No. 09QNET06).

References

[1] T.R.N. Kutty, M. Nayak, J. Alloys Compd. 269 (1998) 75–87.
[2] T. Abritta, F. de Souza Barros, N.T. Melamed, J. Lumin. 33 (1985) 141–146.
[3] N.T. Melamed, F. de Souza Barros, P.J. Viccaro, J.O. Artman, Phys. Rev. B 5 (1972) 3377–3387.
[4] G.T. Pott, B.D. McNicol, J. Chem. Phys. 56 (1972) 5246–5254.
[5] M.W. Parker, H.A. Bothwick, Plant Physiol. 24 (1949) 345.
[6] S. Hashimoto, K. Hattori, K. Inoue, A. Nakahashi, S. Honda, Y. Iwamoto, Mater. Res. Bull. 44 (2009) 70–73.
[7] J. Zhou, Y. Wang, B. Liu, Y. Lu, J. Alloys Compd. 484 (2009) 439–443.
[8] J. Chen, F. Gu, C. Li, Cryst. Growth Des. 8 (2008) 3175–3179.
[9] F. Ren, D. Chen, Opt. Laser Technol. 42 (2010) 110–114.
[10] A. Nag, T.R.N. Kutty, J. Alloys Compd. 354 (2003) 221–231.
[11] J. Niittykoski, T. Aitasalo, J. Hölsä, H. Jungner, M. Lastusaari, M. Parkkinen, M. Tukia, J. Alloys Compd. 374 (2004) 108–111.
[12] K.Y. Jung, H.W. Lee, H.K. Jung, Chem. Mater. 18 (2006) 2249–2255.
[13] L. Vegard, Z. Phys. 5 (1921) 17–26.
[14] H. Riesen, Chem. Phys. Lett. 461 (2008) 218–221.
[15] E.W.J.L. Oomen, K. Van Der Vlist, W.M.A. Smit, G. Blasse, Chem. Phys. Lett. 129 (1996) 9–12.
[16] T. Miyakawa, D.L. Dexter, Phys. Rev. B 1 (1970) 2961–2968.
[17] M.J. Weber, T.E. Varitimos, B.H. Matsinger, Phys. Rev. B 8 (1973) 47–53.